

## Review

# Cytochrome P450-Induced Backbone Rearrangements in Terpene Biosynthesis of Plants

Maximilian Frey <sup>1,2,3,\*</sup> , Christina Marie Jochimsen <sup>1</sup> and Jörg Degenhardt <sup>1</sup> 
<sup>1</sup> Department of Pharmaceutical Biology and Pharmacology, Institute of Pharmacy, Martin Luther University Halle-Wittenberg, Hoher Weg 8, 06120 Halle (Saale), Germany

<sup>2</sup> Department of Cell and Metabolic Biology, Leibniz Institute of Plant Biochemistry, Weinberg 3, 06120 Halle (Saale), Germany

<sup>3</sup> Heidelberg University, Biochemistry Center, 69120 Heidelberg, Germany

\* Correspondence: maximilian.frey@ipb-halle.de or maximilian.frey@bzh.uni-heidelberg.de

## Abstract

Terpenes, the largest class of plant specialized products, are built from C<sub>5</sub> building blocks via terpene synthases and oxidized by cytochrome P450 enzymes (CYPs) for structural diversity. In some cases, CYPs do not simply oxidize the terpene backbone, but induce backbone rearrangements, methyl group shifts, and carbon–carbon (C–C) scissions. Some of these reactions were characterized over 25 years ago, but most of them were reported in recent years, indicating a highly dynamic research area. These reactions are involved in mono-, sesqui-, di- and triterpene metabolism and provide key catalytic steps in the biosynthesis of plant hormones, volatiles, and defense compounds. Many commercially relevant terpenoids require such reaction steps in their biosynthesis such as triptonide (rodent pest management), secoiridoids (flavor determinants), as well as ginkgolides, cardenolides, and sesquiterpene lactones with pharmaceutical potential. Here, we provide a comprehensive overview of the underlying mechanisms.

**Keywords:** P450s; terpenes; rearrangement reactions



Academic Editor: Dae-Yeon Suh

Received: 12 June 2025

Revised: 26 August 2025

Accepted: 27 August 2025

Published: 29 August 2025

**Citation:** Frey, M.; Jochimsen, C.M.; Degenhardt, J. Cytochrome P450-Induced Backbone Rearrangements in Terpene Biosynthesis of Plants. *Molecules* **2025**, *30*, 3540. <https://doi.org/10.3390/molecules30173540>

**Copyright:** © 2025 by the authors. Licensee MDPI, Basel, Switzerland. This article is an open access article distributed under the terms and conditions of the Creative Commons Attribution (CC BY) license (<https://creativecommons.org/licenses/by/4.0/>).

## 1. Introduction: The Modular Biosynthesis of Terpenes

Terpenes are the largest class of plant specialized products with an overwhelming diversity of structures [1]. This diversity is based on precursors derived from the same C<sub>5</sub> building blocks and a modular biosynthesis of (1) generation of a terpene backbone by terpene synthases and (2) oxidation of the backbone by cytochrome P450 enzymes (CYPs) (Figure 1) [2]. Cytochrome P450 enzymes typically introduce molecular oxygen into the terpene backbone, thereby leading to the decoration of these backbones with hydroxy-, keto-, acid-, epoxy- and lactone groups [3]. Hydroxy groups often function as anchors that allow the esterification with organic acids, sugars, and other moieties. However, CYPs can carry out reactions other than these typical backbone decorations in almost all classes of terpenes (Figure 1) leading to modified terpene backbones.

The CYP-induced modifications in plant terpene backbones include C–C cleavage (Figure 2A) resulting in the cleavage of alkyl groups (I) [4], or the opening of one (II) [5] or two (III) [6] rings. CYP-induced rearrangement reactions (Figure 2B) can include ring contraction (IV) [7,8] and transannular cyclization (V) [9], which can also occur in combination with C–C scission (VI) [10]. Most recently, group shifts were observed to be induced by CYPs (Figure 2C), such as the shift in a methyl- (VII) [11] or an alkyl group (VIII) [6] along a ring. These CYP-induced terpene backbone modifications occur on mono-, di-, sesqui-,

and triterpenes, and the CYPs carrying out these reaction types are members of a diverse array of CYP families (Table 1).

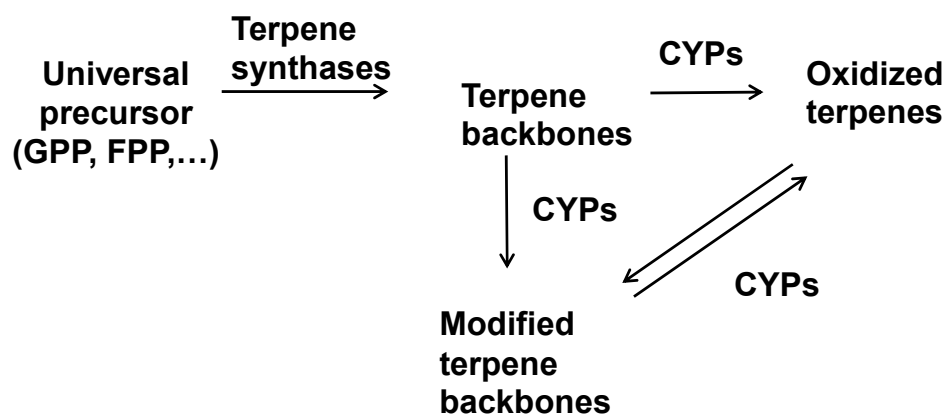


**Figure 1.** General scheme for the biosynthesis of plant terpenes.

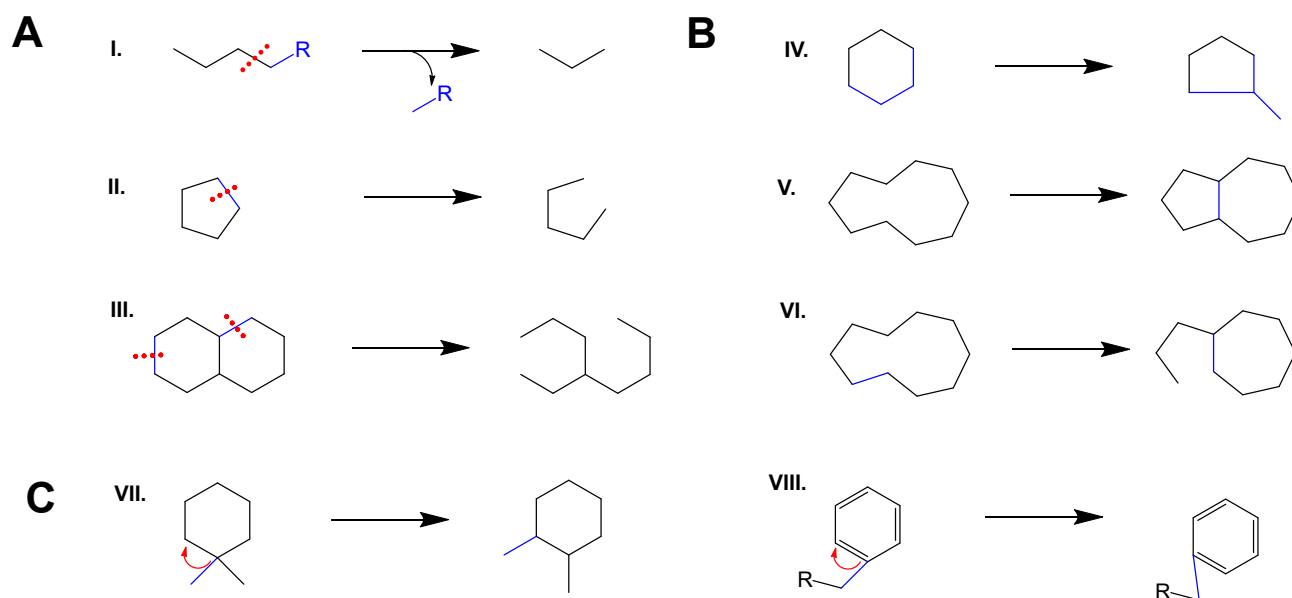


**Figure 2.** Types of CYP-induced terpene backbone modifications. (A) C–C scission leading to cleavage (I), or the opening of one (II) or two rings (III). (B) Rearrangements: ring contraction (IV), transannular cyclization without (V), and with ring opening (VI). (C) Group shifts: Methyl (VII) and alkyl (VIII) group shifts.

**Table 1.** Reaction types and CYP subfamilies.

| Type | Reactions (References)  | P450 Subfamily | Enzymes              | Number * | Terpene Substrate |
|------|---|----------------|----------------------|----------|-------------------|
| I    | C–C scission, cleaving of C1 unit, demethylation of obtusifolioside ([12,13])   | CYP51G         |                      | 3        | Triterpene        |
| I    | C–C scission, cleave of a four (-C <sub>4</sub> ) unit from sesquiterpene or diterpene precursors to produce C11- or C16-homoterpenes ([4,14–17]) | CYP92C         | CYP92C5,6            | 2        | Sesqui-/Diterpene |
|      |   | CYP82D/G/L     |                      | 4        |                   |
| I    | C–C scission, cleaving of side chains of various lengths (C <sub>6</sub> –C <sub>8</sub> ) to produce cardenolides via pregnenolone ([18])        |                |                      | 3        | Triterpene        |
| II   | C–C scission in the formation of secoiridoids ([5])   | CYP72A         | SLAS, SLS, SXS, OMES | 4        | Monoterpene       |
| III  | C–C scission, ring opening of ring A and ring B in levopimaradiene ([6])  | CYP7005C       | CYP7005C1/C3         | 2        | Diterpene         |
| IV   | Ring contraction of kaurenoic acid B ring in the gibberellin biosynthesis ([8])   | CYP88A         | KAO                  | >10      | Diterpene         |
| V    | Ring rearrangement, transannular cyclization, formation of 6,7-trans guaianolides ([9,19])  | CYP71BZ        | KLS                  | 4        | Sesquiterpene     |
| VI   | Ring rearrangement, transannular cyclization, formation of 7,8-trans xanthanolides ([10])   | CYP71DD        | CYP72DD1             | 1        | Sesquiterpene     |
| VII  | Methyl group shift, 18 (4 → 3), via Wagner–Meerwein rearrangement ([11])  | CYP71BE        |                      | 2        | Diterpene         |
| VIII | Alkyl group shift along aromatic ring from C8 to C9 of ginkgosinic acid B ([6])   | CYP867K        | GbCYP867K1           | 1        | Diterpene         |

Note: In almost all cases, the CYP subfamilies include enzymes with various other substrate and reaction types. \* Number of enzymes catalyzing this reaction.

## 2. C–C Scission and Ring Opening

An essential step in plant sterol metabolism is the demethylation ( $-C_1$ ) of obtusifoliosol (1) to  $4\alpha$ -methyl-ergosta-8,24(24<sup>1</sup>)-dien-3 $\beta$ -ol (2) by an obtusifoliosol  $14\alpha$ -demethylase from the CYP51G subfamily [12,13] (Figure 3A). A CYP51G enzyme from a wild potato species (*Solanum chacoense*) accepted both obtusifoliosol and lanosterol as substrates for C14-demethylation [20] and the homologous enzyme from maize accepted alternative substrates such as  $24\alpha(28)$ -dihydro-obtusifoliosol and  $24,(25)$ -dihydro-31-norlanosterol [21]. CYPs also play a key role in the formation of homoterpenes (Figure 3B), that is often herbivore-induced: CYP92C5 in maize (*Zea mays*) can cleave off a four ( $-C_4$ ) unit from the sesquiterpene ( $C_{15}$ ) precursor (*E*)-nerolidol (3) to yield the homoterpene (*E*)-3,8-dimethyl-1,4,7-nonatriene (DMNT) (4) ( $C_{11}$ ). Also, CYP92C5 (and CYP92C6) can convert the diterpene precursor (*E,E*)-geranylinalool (5) ( $C_{20}$ ) to (*E,E*)-4,8,12-trimethyltrideca-1,3,7,11-tetraene (TMTT) (6) ( $C_{16}$ ) [4]. The exact reaction mechanism and the fate of the cleaved carbon atoms have not been determined. In triterpene ( $C_{30}$ ) metabolism, there are not only examples of CYPs that induce the cleavage of a methyl group ( $C_1$ ), but also CYPs that induce the cleavage of ( $C_6$ – $C_8$ ) sterol side chains, which is required for the biosynthesis of cardenolides. Kunert et al. [18] characterized enzymes from the CYP87A1 subfamily that were able to convert cholesterol (7) ( $C_{27}$ ), campesterol (8) ( $C_{28}$ ), and  $\beta$ -sitosterol (9) ( $C_{29}$ ) to pregnenolone (10) ( $C_{21}$ ), cleaving off side chains of various lengths ( $C_6$ – $C_8$ ) (Figure 3C). The authors identified the corresponding CYP enzymes from the phylogenetically distant plants foxglove (*Digitalis purpurea*), treacle-mustard (*Erysimum cheiranthoides*), and giant milkweed (*Calotropis procera*). Based on comparative docking studies, the authors propose a mechanism similar to that of HsCYP11A1, the cholesterol side-chain cleavage enzyme in humans (*Homo sapiens*), in which two hydroxylation reactions of cholesterol at C20 and C22 are followed by C20–C22 cleavage of 20,22-dihydroxycholesterol [18,22].

The biosynthesis of monoterpene ( $C_{10}$ ) iridoids including the formation of the different stereochemical orientations that can be realized in nature is well understood in several plant species. A subgroup of these, the secoiridoids, require a ring-opening mechanism that can be carried out by various CYP enzymes. One recent example was reported by Rodriguez-Lopez et al. [5] who described the oxidative C–C cleavages of ketologanin (11) to form either secoxyloganin (12) or oleoside methyl ester (OME) (13) catalyzed by CYP72 enzymes (Figure 3D) in olive (*Olea europaea*). This oxidative C–C cleavage (Figure 3D) in the pathway to secoiridoids is carried out by enzymes from the CYP72A subfamily. In the early 90s, Vetter et al. (1992) [23] described the first CYP72 enzyme CYP72A1 in Madagascar periwinkle (*Catharanthus roseus*), which was assumed to play a role in iridoid metabolism, but the exact enzymatic function remained unclear. Using microsomal preparations from Japanese honeysuckle (*Lonicera japonica*), Yamamoto et al. showed that the C–C cleavage en route from loganin to secologanin is carried out by a P450 enzyme [24]. They described this enzyme as secologanin synthase (SLS) and proposed mechanisms for this P450-induced C–C cleavage. Later, Irmeler et al. showed that the function of CYP72A1 was the oxidative C–C cleavage of loganin to secologanin [25]. By now, four such reactions by CYP72 enzymes have been characterized in detail in three plant species: 1. conversion of loganic acid to secologanic acid in *Camptotheca acuminata* by secologanic acid synthases (SLASs) (CYP72A565, CYP72A610) [26]; 2. conversion of loganin to secologanin in Madagascar periwinkle (*Catharanthus roseus*) by CrSLS [25]; 3. conversion of ketologanin (11) to either secoxyloganin (12); or 4. conversion of ketologanin to OME (13) in olive (*Olea europaea*) [5]. Interestingly, CYP enzymes from the CYP72A subfamily are involved in a wide range of terpenoid biochemical pathways, such as monoterpene (iridoids), diterpene (gibberellin), and triterpenoid (steroids, avenacin) biosynthesis. While elucidating the metabolic pathways to ginkgolides in ginkgo, Forman et al. [6] observed an intriguing CYP reaction: an

2 $\alpha$ -hydroxylation of levopimaradiene (**14**) with a subsequent opening of ring A and B of levopimaradiene backbone ultimately yielding ginkgosinic acid A (**15**) by *Gb*CYP7005C1.

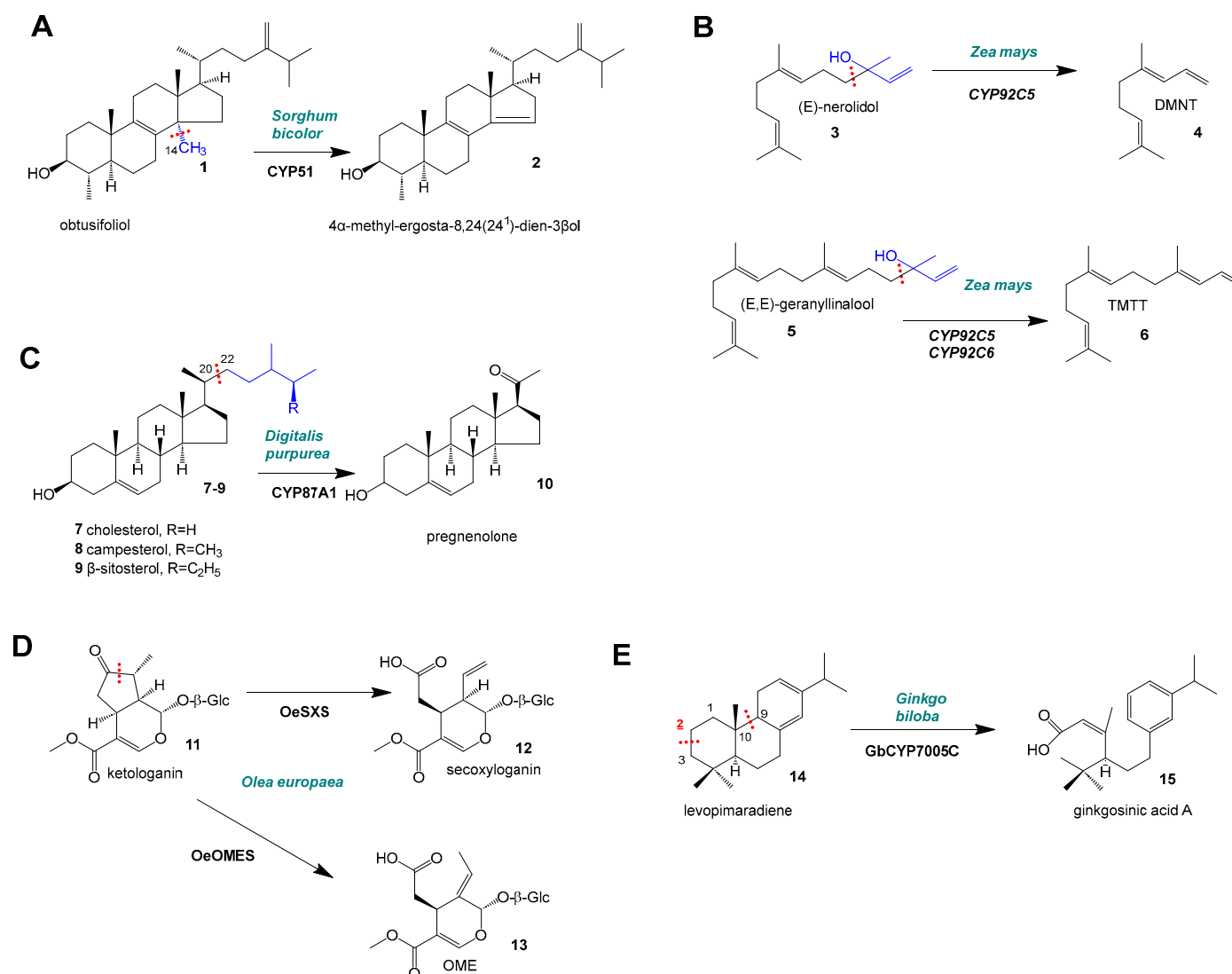


**Figure 3.** P450-induced C–C scission reactions resulting in ring opening and cleavage of side chains. (A) CYP51 reaction in *Sorghum bicolor*; (B) CYP92C5/6 reactions in *Zea mays*; (C) CYP87A1 reaction in *Digitalis purpurea*; (D) Reaction of OeSXS and OeOMES in *Olea europaea*; (E) CYP7005C reaction in *Ginkgo biloba*. Red, underlined: position of carbon atom that is initially oxidized. Blue: part of the molecule that is cleaved off.

### 3. Ring Rearrangements of the Backbones (IV)–(VI)

One of the most conserved terpenoid pathways in land plants is the formation of gibberellin plant hormones. A key step in this pathway is the conversion of kaurenoic acid (**16**) to GA<sub>12</sub> (**17**) by kaurenoic acid oxidases (KAOs) from CYPs of the CYP88A subfamily [7,8] (Figure 4A). This three-step reaction proceeds via 7-hydroxy kaurenoic acid and 7-keto kaurenoic acid. In the final step, the formation of an acid group at C7 and the ring B contraction from C6 to C5 are catalyzed.

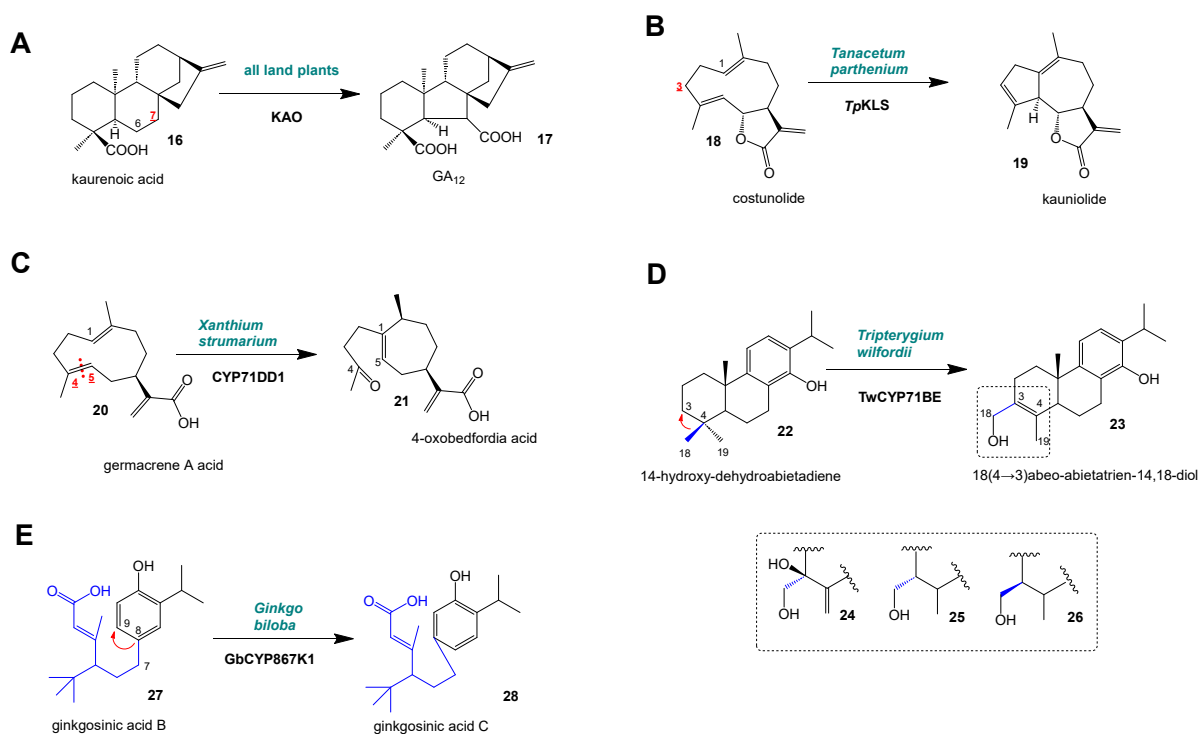


**Figure 4.** P450-induced rearrangement reactions and alkyl group shifts in plant terpene biosynthesis. (A) Kaurene oxidase (KAO) reaction in all land plants; (B) KLS reaction in *Tanacetum parthenium*; (C) CYP71DD1 reaction in *Xanthium strumarium*; (D) CYP71BE reaction in *Tripterygium wilfordii*; (E) CYP867K1 reaction in *Ginkgo biloba*. Red, underlined: position of carbon atom that is initially oxidized. Blue: Side chain that was shifted by the P450 reaction.

In a large subclass of sesquiterpenes (C<sub>15</sub>), the sesquiterpene lactones (STLs), CYPs contribute to the formation of specific backbones. Not all terpene structures observed in nature are the result of terpene synthase reactions. For instance, the class of STLs with >5000 compounds contains dozens of backbone types, most of which are believed to arise from a common germacrene backbone ring [27,28]. The formation of guaianolides is enabled by kauniolide synthases (KLSs) that convert costunolide (18) to kauniolide (19) in feverfew (*Tanacetum parthenium*) and chicory (*Cichorium intybus*) [9,19,29] (Figure 4B). The formation of xanthanolide STL is initiated by the conversion of germacrene A acid (20) to 4-oxobedfordia acid (21) by CYP71DD1 in *Xanthium strumarium* [10] (Figure 4C).

#### 4. Methyl/Alkyl Group Shifts

In diterpene (C<sub>20</sub>) biosynthesis, many unusual P450 reactions are reported. Hansen et al. [11] observed a CYP-induced shift in a methyl (C<sub>1</sub>) group along the ring of a diterpene in the thunder god vine (*Tripterygium wilfordii*) biosynthetic pathway to triptonide. Two enzymes from the CYP71BE subfamily convert 14-hydroxy-dehydroabietadiene (22) to 18 (4 → 3) abeo-abietatrien-14,18-diol (23), shifting the C18 methyl group from C4 to C3 along the A ring (Figure 4D). These CYP reactions resulted in a variety of products with a shifted methyl group (24–26). In a later step of ginkgolide biosynthesis, ginkgosinic acid B (27) is converted to ginkgosinic acid C (28) by CYP867K1 (Figure 4E). Intriguingly, CYP867K1 shifts the branched C<sub>11</sub> side chain from C8 to C9 along the C ring.

## 5. Underlying Mechanisms

### 5.1. Ring Rearrangement Mechanisms

In the biosynthesis of gibberellins (diterpenes) KAO converts ent-kaurenoic acid (**16**) to GA<sub>12</sub> (**17**) in three steps without intermediate release. *Ent*-Kaurenoic acid undergoes C7 hydroxylation, ring contraction, then oxidation to GA<sub>12</sub> [7,8,30].

In sesquiterpene biosynthesis the germacrene backbone is prone to acid-induced rearrangements to eudesmanolides and heat-induced Cope rearrangements to elemenes [28,31], which can be artifacts of the analytical technique. However, this formation of eudesmanolide backbones after P450 oxidation was recently observed in planta [32]. Two major STL backbone types, the xanthanolides and the guaianolides, were recently shown to be derived from the common germacrenolide precursor germacrene A acid (GAA) (**20**). In the case of the guaianolide STL kauniolide a “post-lactone” pathway requires the lactone formation from GAA to costunolide (**18**), before the conversion of the backbone. Liu et al. [9] discovered that the enzyme *Tp*KLS can convert costunolide (**18**) into 3 $\alpha$ -hydroxycostunolide (**29**), which is subsequently converted into kauniolide (**19**) (Figure 5).

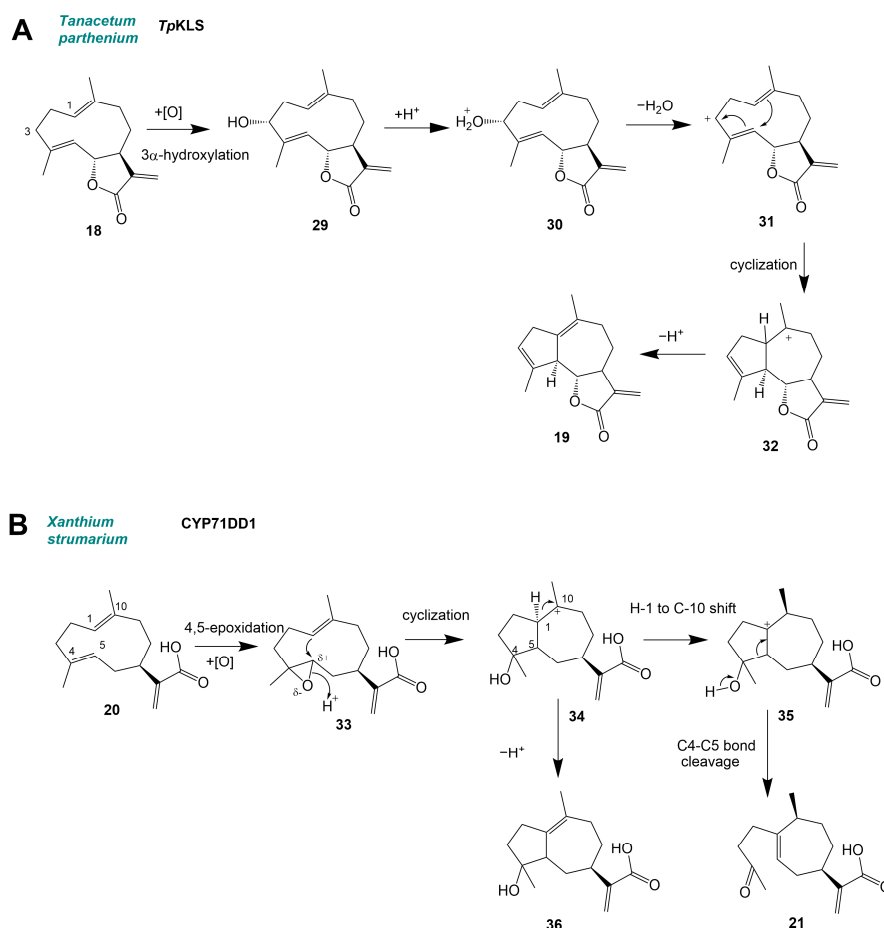


**Figure 5.** P450-induced rearrangement reactions of sesquiterpenes. (A) Kauniolide synthase (modified from Liu et al., 2018) and (B) CYP71DD1 (modified from Li et al., 2024) [9,10].

In the proposed mechanism of the backbone rearrangement, the 3 $\alpha$ -hydroxy group of this intermediate is protonated (**30**) [9]. The loss of a water molecule then leads to a C3 carbocation (**31**) that induces the ring rearrangement to (**32**). After protonation kauniolide (**19**) is formed [9]. Recently, homologous KLS enzymes belonging to the same P450 subfamily were characterized in chicory (*Cichorium intybus*), albeit with a relatively low amino acid identity [19,29]. All kauniolide synthases characterized thus far belong to the CYP71BZ subfamily. In the “pre-lactone” pathway recently described by Li et al. [10], the



backbone conversion occurs before the formation of a lactone ring, challenging previous assumptions [27] about the formation of *Asteraceae* STL. In *Xanthium strumarium*, GAA is converted to 4-oxobedfordia acid (21) by CYP71DD1, ultimately leading to the formation of the 7,8-cis-xanthanolide STLs 8-epi-xanthatin and tomentosin [10]. Based on previously reported mechanisms for the formation of xanthanolides from the 4,5-epoxide parthenolide [33], the authors suggest a mechanism that includes oxygenation, cyclization, and C–C bond scission: In the first step, CYP71DD1 converts GAA (8) to 4,5-epoxy-GAA (33). Starting from 4,5-epoxy-GAA, a 1,10-double bond attack initiates transannular cyclization to intermediate (34), followed by either cleavage to (21) or cyclization to (36) [10]. A similar mechanism could be responsible for the formation of 7,8-cis lactone guaianolide STL. The CYP71DD subfamily appears to be specific to *Asteraceae* STL metabolism [28], where enzymes from this subfamily typically introduce hydroxy groups into oxidized sesquiterpene backbones such as germacrene A acid (20) (CYP71DD1), kauniolide (19) (CYP71DD5) [9], 8 $\beta$ -hydroxygermacrene A acid (CYP71DD6) [32], or 8-deoxylactucin [34] (CYP71DD33).

## 5.2. Cleavage Mechanisms

The formal by-product of the one-step oxidative degradation (Figure 6A) of (*E*)-nerolidol (12) to DMNT (13) is but-3-ene-2-one (methyl vinyl ketone) (37) (C<sub>4</sub>), but it has not been detected as a by-product of homoterpene formation [35,36]. An alternative two-step reaction mechanism has been postulated, that proceeds via the ketone intermediates geranylacetone (38) and farnesylacetone, respectively, (Figure 6B) [36]. In this mechanism, two carbon (C<sub>2</sub>) units would be cleaved, but experimental evidence for it remains inconclusive. Small amounts of geranylacetone have been detected in DMNT-containing volatile blends [37], and geranylacetone was converted in feeding experiments with lima bean (*Phaseolus lunatus*) and purple magnolia (*Magnolia liliiflora nigra*) [36]. In contrast, the ketone intermediates were not detected in assays with the thale cress (*Arabidopsis thaliana*) CYP82G1 and they were shown to be inefficient substrates for the conversion to homoterpenes catalyzed by this enzyme [15]. Even though the reaction mechanism requires further investigation, some mechanistic aspects have already been elucidated, namely, that it proceeds via *syn*-elimination of the oxygen-carrying group with a hydrogen atom of the allylic  $\beta$ -carbon [38]. In rice, OsCYP92C21 produces both DMNT and TMTT [39]. This reaction can also be carried out by enzymes from the CYP82 family: CYP82D in tea (*Camellia sinensis*) [14], CYP82G in thale cress (*A. thaliana*) [15], and CYP82L in cotton (*Gossypium hirsutum*) [16] and orange (*Citrus sinensis*) [17].

Rodriguez-Lopez et al. [5] have suggested reaction mechanisms for the CYP-catalyzed oxidative cleavages en route to secoiridoids in olive (Figure S1). CrSLS, which oxidizes loganin (39) via (40,41) to secologanin (42) (Figure S1A), follows a similar mechanism as OeSXS, which oxidizes ketologanin (5) via (43,44) to secoxyloganin (6) (Figure S1B) while OeOMES converts ketologanin (5) to OME (7) via (45,46) (Figure S1C). The authors speculate that the stereochemistry of the hydroxyl group in position 7 of loganin determines the orientation of the substrate in the CrSLS binding site, such that the hydrogen of C10 can be abstracted by the iron cofactor, ultimately leading to secologanin [24] (Figure S1A).

GbCYP7005C1/7005C3 cleave two C–C bonds in levopimaradiene (14), with a radical shift from C3 to C1, preserving the tert-butyl group (Figure S1D) via intermediates (47–49). As proposed by Schwarz and Arigoni [40], a hydrogen shift enables oxygen rebound and subsequent rearrangement via aromatization, dehydration, and heterolytic cleavage (Figure S1C) via intermediates (50,51) to ginkgosinic acid A (15) [6].



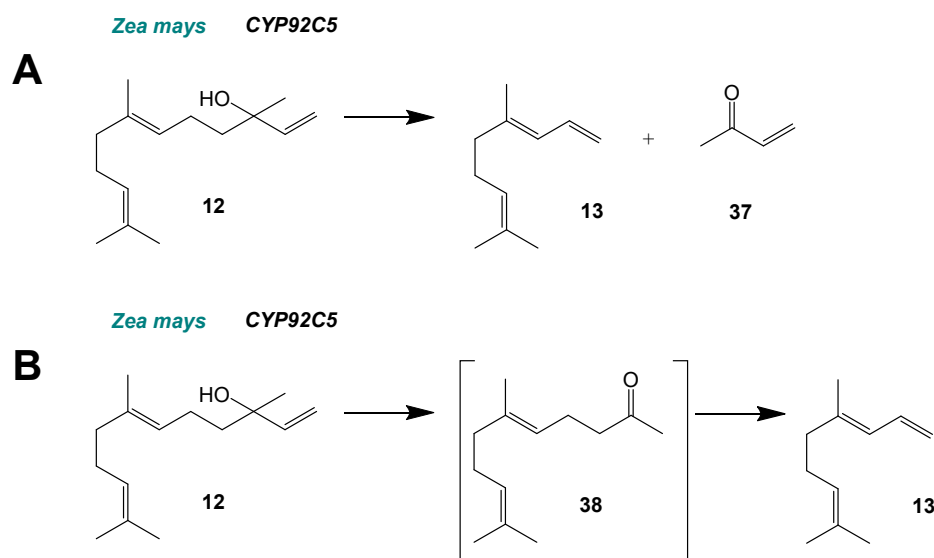


**Figure 6.** Side chain cleavage by CYP92 enzymes. **(A)** Single step fragmentation. **(B)** Two-step fragmentation proceeding via the consecutive loss of two C2 moieties. Figure modified from Lee et al. (2010) [15].

### 5.3. Group Shift Mechanisms

The C7–C8 to C7–C9 shift from ginkgosinic acid B (**27**) to ginkgosinic acid C (**28**) may proceed via a dienone-phenol NIH rearrangement via intermediate (**52**) (Figure S2A). Alternatively, epoxidation with acid-catalyzed opening and alkyl migration via intermediates (**53–55**) yields ginkgosinoic acid C. In the conversion of 14-hydroxy-dehydroabietadiene (**22**) to multiple products (**23–26**; **56–58**) (Figure S2B), a hypothetical Wagner–Meerwein rearrangement explains the C18 to C3 methyl shift in the abietane backbone [11].

## 6. Conclusions and Perspectives

In recent years, there has been a growing number of reports of unusual P450 reactions. These observations may pave the way forward for the elucidation of metabolic pathways with so far elusive mechanisms. One example is the furan ring formation in cafestol biosynthesis, which requires a methyl group shift in the kaurene backbone, similar to what has been observed in triptolide biosynthesis. It would be very interesting to screen P450s with non-canonical reactions in high-throughput assays for alternative substrates to exploit their unique biosynthetic activity for other chemical reactions. Site-directed mutagenesis studies guided by substrate docking as well as feeding assays with hypothesized intermediates can provide a more detailed understanding of the sequence of reactions carried out by these P450s. With the advancements in genome sequencing, high-throughput testing, as well as metabolomics and transcriptomics on a cellular level, we expect the elucidation of additional P450-induced rearrangement reactions in the future.

**Supplementary Materials:** The following supporting information can be downloaded at <https://www.mdpi.com/article/10.3390/molecules30173540/s1>, Figure S1: Pathways for C–C scission by CYP enzymes; Figure S2: CYP-induced group shifts.

**Author Contributions:** Conceptualization, M.F.; writing—original draft preparation, M.F., C.M.J. and J.D.; writing—review and editing, M.F.; visualization, M.F.; supervision, M.F. All authors have read and agreed to the published version of the manuscript.

**Funding:** This research received no external funding.

**Institutional Review Board Statement:** Not applicable.

**Informed Consent Statement:** Not applicable.

**Data Availability Statement:** No new data were created or analyzed in this study. Data sharing is not applicable to this article.

**Conflicts of Interest:** The author declares no conflicts of interest.

## References

- Wink, M. Introduction: Biochemistry, Physiology and Ecological Functions of Secondary Metabolites. In *Annual Plant Reviews Volume 40: Biochemistry of Plant Secondary Metabolism*; Blackwell Publishing Ltd.: Hoboken, NJ, USA, 2010; pp. 1–19.
- Frey, M.; Bathe, U.; Meink, L.; Balcke, G.U.; Schmidt, J.; Frolov, A.; Soboleva, A.; Hassanin, A.; Davari, M.D.; Frank, O.; et al. Combinatorial biosynthesis in yeast leads to over 200 diterpenoids. *Metab. Eng.* **2024**, *82*, 193–200. [\[CrossRef\]](#) [\[PubMed\]](#)
- Pateraki, I.; Heskes, A.M.; Hamberger, B. Cytochromes P450 for terpene functionalisation and metabolic engineering. *Adv. Biochem. Eng. Biotechnol.* **2015**, *148*, 107–139. [\[CrossRef\]](#) [\[PubMed\]](#)
- Richter, A.; Schaff, C.; Zhang, Z.; Lipka, A.E.; Tian, F.; Köllner, T.G.; Schnee, C.; Preiß, S.; Irmisch, S.; Jander, G.; et al. Characterization of Biosynthetic Pathways for the Production of the Volatile Homoterpenes DMNT and TMTT in *Zea mays*. *Plant Cell* **2016**, *28*, 2651–2665. [\[CrossRef\]](#)
- Rodríguez-López, C.E.; Hong, B.; Paetz, C.; Nakamura, Y.; Koudounas, K.; Passeri, V.; Baldoni, L.; Alagna, F.; Calderini, O.; O'Connor, S.E. Two bi-functional cytochrome P450 CYP72 enzymes from olive (*Olea europaea*) catalyze the oxidative C–C bond cleavage in the biosynthesis of secoxy-iridoids—Flavor and quality determinants in olive oil. *New Phytol.* **2021**, *229*, 2288–2301. [\[CrossRef\]](#)
- Forman, V.; Luo, D.; Geu-Flores, F.; Lemcke, R.; Nelson, D.R.; Kampranis, S.C.; Staerk, D.; Möller, B.L.; Pateraki, I. A gene cluster in *Ginkgo biloba* encodes unique multifunctional cytochrome P450s that initiate ginkgolide biosynthesis. *Nat. Commun.* **2022**, *13*, 5143. [\[CrossRef\]](#)
- Helliwell, C.A.; Poole, A.; James Peacock, W.; Dennis, E.S. Arabidopsis *ent*-Kaurene Oxidase Catalyzes Three Steps of Gibberellin Biosynthesis. *Plant Physiol.* **1999**, *119*, 507–510. [\[CrossRef\]](#)
- Helliwell, C.A.; Chandler, P.M.; Poole, A.; Dennis, E.S.; Peacock, W.J. The CYP88A cytochrome P450, *ent*-kaurenoic acid oxidase, catalyzes three steps of the gibberellin biosynthesis pathway. *Proc. Natl. Acad. Sci. USA* **2001**, *98*, 2065–2070. [\[CrossRef\]](#)
- Liu, Q.; Beyraghdar Kashkooli, A.; Manzano, D.; Pateraki, I.; Richard, L.; Kolkman, P.; Lucas, M.F.; Guallar, V.; de Vos, R.C.H.; Franssen, M.C.R.; et al. Kauniolide synthase is a P450 with unusual hydroxylation and cyclization-elimination activity. *Nat. Commun.* **2018**, *9*, 4657. [\[CrossRef\]](#)
- Li, C.; Li, Y.; Wang, J.; Lu, F.; Zheng, L.; Yang, L.; Sun, W.; Ro, D.-K.; Qu, X.; Wu, Y.; et al. An independent biosynthetic route to frame a xanthanolide-type sesquiterpene lactone in Asteraceae. *Plant J.* **2024**, *121*, e17199. [\[CrossRef\]](#)
- Hansen, N.L.; Kjaerulff, L.; Heck, Q.K.; Forman, V.; Staerk, D.; Möller, B.L.; Andersen-Ranberg, J. *Tripterygium wilfordii* cytochrome P450s catalyze the methyl shift and epoxidations in the biosynthesis of triptonide. *Nat. Commun.* **2022**, *13*, 5011. [\[CrossRef\]](#) [\[PubMed\]](#)
- Bak, S.; Kahn, R.A.; Olsen, C.E.; Halkier, B.A. Cloning and expression in *Escherichia coli* of the obtusifolioside 14 $\alpha$ -demethylase of *Sorghum bicolor* (L.) Moench, a cytochrome P450 orthologous to the sterol 14 $\alpha$ -demethylases (CYP51) from fungi and mammals. *Plant J.* **1997**, *11*, 191–201. [\[CrossRef\]](#) [\[PubMed\]](#)
- Burger, C.; Rondet, S.; Benveniste, P.; Schaller, H. Virus-induced silencing of sterol biosynthetic genes: Identification of a *Nicotiana tabacum* L. obtusifolioside-14 $\alpha$ -demethylase (CYP51) by genetic manipulation of the sterol biosynthetic pathway in *Nicotiana benthamiana* L. *J. Exp. Bot.* **2003**, *54*, 1675–1683. [\[CrossRef\]](#) [\[PubMed\]](#)
- Jing, T.; Du, W.; Gao, T.; Wu, Y.; Zhang, N.; Zhao, M.; Jin, J.; Wang, J.; Schwab, W.; Wan, X.; et al. Herbivore-induced DMNT catalyzed by CYP82D47 plays an important role in the induction of JA-dependent herbivore resistance of neighboring tea plants. *Plant Cell Environ.* **2021**, *44*, 1178–1191. [\[CrossRef\]](#) [\[PubMed\]](#)
- Lee, S.; Badiyan, S.; Bevan, D.R.; Herde, M.; Gatz, C.; Tholl, D. Herbivore-induced and floral homoterpene volatiles are biosynthesized by a single P450 enzyme (CYP82G1) in *Arabidopsis*. *Proc. Natl. Acad. Sci. USA* **2010**, *107*, 21205–21210. [\[CrossRef\]](#)
- Liu, D.; Huang, X.; Jing, W.; An, X.; Zhang, Q.; Zhang, H.; Zhou, J.; Zhang, Y.; Guo, Y. Identification and functional analysis of two P450 enzymes of *Gossypium hirsutum* involved in DMNT and TMTT biosynthesis. *Plant Biotechnol. J.* **2018**, *16*, 581–590. [\[CrossRef\]](#)
- Sun, X.; Hu, C.; Yi, G.; Zhang, X. Identification and characterization of two P450 enzymes from *Citrus sinensis* involved in TMTT and DMNT biosyntheses and Asian citrus psyllid defense. *Hortic. Res.* **2024**, *11*, uhae037. [\[CrossRef\]](#)
- Kunert, M.; Langley, C.; Lucier, R.; Ploss, K.; Rodríguez López, C.E.; Serna Guerrero, D.A.; Rothe, E.; O'Connor, S.E.; Sonawane, P.D. Promiscuous CYP87A enzyme activity initiates cardenolide biosynthesis in plants. *Nat. Plants* **2023**, *9*, 1607–1617. [\[CrossRef\]](#)
- Cankar, K.; Hakkert, J.C.; Sevenier, R.; Campo, E.; Schipper, B.; Papastolopoulou, C.; Vahabi, K.; Tissier, A.; Bundock, P.; Bosch, D. CRISPR/Cas9 targeted inactivation of the kauniolide synthase in chicory results in accumulation of costunolide and its conjugates in taproots. *Front. Plant Sci.* **2022**, *13*, 940003. [\[CrossRef\]](#)

20. O'Brien, M.; Chantha, S.-C.; Rahier, A.; Matton, D.P. Lipid Signaling in Plants. Cloning and Expression Analysis of the Obtusifoliosol 14 $\alpha$ -Demethylase from *Solanum chacoense* Bitt., a Pollination- and Fertilization-Induced Gene with Both Obtusifoliosol and Lanosterol Demethylase Activity. *Plant Physiol.* **2005**, *139*, 734–749. [\[CrossRef\]](#)
21. Taton, M.; Rahier, A. Properties and structural requirements for substrate specificity of cytochrome P-450-dependent obtusifoliosol 14  $\alpha$ -demethylase from maize (*Zea mays*) seedlings. *Biochem. J.* **1991**, *277*, 483–492. [\[CrossRef\]](#)
22. Strushkevich, N.; MacKenzie, F.; Cherkasova, T.; Grabovec, I.; Usanov, S.; Park, H.W. Structural basis for pregnenolone biosynthesis by the mitochondrial monooxygenase system. *Proc. Natl. Acad. Sci. USA* **2011**, *108*, 10139–10143. [\[CrossRef\]](#)
23. Vetter, H.-P.; Mangold, U.; Schro, G.; Marner, F.-J.; Werck-Reichhart, D.; Schro, J. Molecular Analysis and Heterologous Expression of an Inducible Cytochrome P-450 Protein from Periwinkle (*Catharanthus roseus* L.). *Plant Physiol.* **1992**, *100*, 998–1007. [\[CrossRef\]](#)
24. Yamamoto, H.; Katano, N.; Ooi, A.; Inoue, K. Secologanin synthase which catalyzes the oxidative cleavage of loganin into secologanin is a cytochrome P450. *Phytochemistry* **2000**, *53*, 7–12. [\[CrossRef\]](#)
25. Irmeler, S.; Schroder, G.; St-Pierre, B.; Crouch, N.P.; Hotze, M.; Schmidt, J.; Strack, D.; Matern, U.; Schroder, J. Indole alkaloid biosynthesis in *Catharanthus roseus*: New enzyme activities and identification of cytochrome P450 CYP72A1 as secologanin synthase. *Plant J.* **2000**, *24*, 797–804. [\[CrossRef\]](#)
26. Yang, Y.; Ding, L.; Zhou, Y.; Guo, Z.; Yu, R.; Zhu, J. Establishment of recombinant *Catharanthus roseus* stem cells stably overexpressing ORCA4 for terpenoid indole alkaloids biosynthesis. *Plant Physiol. Biochem.* **2023**, *196*, 783–792. [\[CrossRef\]](#) [\[PubMed\]](#)
27. Seaman, F.C. Sesquiterpene lactones as taxonomic characters in the asteraceae. *Bot. Rev.* **1982**, *48*, 121–594. [\[CrossRef\]](#)
28. Frey, M.; Vahabi, K.; Cankar, K.; Lackus, N.D.; Padilla-Gonzalez, F.; Ro, D.-K.; Rieseberg, L.; Spring, O.; Tissier, A. Sesquiterpene Lactones—Insights into Biosynthesis, Regulation and Signalling Roles. *Crit. Rev. Plant Sci.* **2024**, *43*, 131–157. [\[CrossRef\]](#)
29. De Bruyn, C.; Ruttink, T.; Lacchini, E.; Rombauts, S.; Haegeman, A.; De Keyser, E.; Van Poucke, C.; Desmet, S.; Jacobs, T.B.; Eeckhaut, T.; et al. Identification and characterization of CYP71 subclade cytochrome P450 enzymes involved in the biosynthesis of bitterness compounds in *Cichorium intybus*. *Front. Plant Sci.* **2023**, *14*, 1200253. [\[CrossRef\]](#) [\[PubMed\]](#)
30. Hedden, P. The Current Status of Research on Gibberellin Biosynthesis. *Plant Cell Physiol.* **2020**, *61*, 1832–1849. [\[CrossRef\]](#)
31. Frey, M. Traps and Pitfalls-Unspecific Reactions in Metabolic Engineering of Sesquiterpenoid Pathways. *Molecules* **2020**, *25*, 1935. [\[CrossRef\]](#)
32. Frey, M.; Schmauder, K.; Pateraki, I.; Spring, O. Biosynthesis of Eupatolide-A Metabolic Route for Sesquiterpene Lactone Formation Involving the P450 Enzyme CYP71DD6. *ACS Chem. Biol.* **2018**, *13*, 1536–1543. [\[CrossRef\]](#)
33. Castaneda-Acosta, J.; Fischer, N.H.; Vargas, D. Biomimetic transformations of parthenolide. *J. Nat. Prod.* **1993**, *56*, 90–98. [\[CrossRef\]](#)
34. Cankar, K.; Hakkert, J.C.; Sevenier, R.; Papastolopoulou, C.; Schipper, B.; Baixinho, J.P.; Fernández, N.; Matos, M.S.; Serra, A.T.; Santos, C.N.; et al. Lactucin Synthase Inactivation Boosts the Accumulation of Anti-inflammatory 8-Deoxylactucin and Its Derivatives in Chicory (*Cichorium intybus* L.). *J. Agric. Food Chem.* **2023**, *71*, 6061–6072. [\[CrossRef\]](#)
35. Boland, W.; Gäbler, A. Biosynthesis of Homoterpenes in Higher Plants. *Helv. Chim. Acta* **1989**, *72*, 247–253. [\[CrossRef\]](#)
36. Gäbler, A.; Boland, W.; Preiss, U.; Simon, H. Stereochemical Studies on Homoterpene Biosynthesis in Higher Plants; Mechanistic, Phylogenetic, and Ecological Aspects. *Helv. Chim. Acta* **1991**, *74*, 1773–1789. [\[CrossRef\]](#)
37. Knudsen, J.T.; Eriksson, R.; Gershenzon, J.; Ståhl, B. Diversity and distribution of floral scent. *Bot. Rev.* **2006**, *72*, 1. [\[CrossRef\]](#)
38. Boland, W.; Gäbler, A.; Gilbert, M.; Feng, Z. Biosynthesis of C11 and C16 homoterpenes in higher plants; stereochemistry of the C–C-bond cleavage reaction. *Tetrahedron* **1998**, *54*, 14725–14736. [\[CrossRef\]](#)
39. Li, W.; Wang, L.; Zhou, F.; Li, C.; Ma, W.; Chen, H.; Wang, G.; Pickett, J.A.; Zhou, J.-J.; Lin, Y. Overexpression of the homoterpene synthase gene, OsCYP92C21, increases emissions of volatiles mediating tritrophic interactions in rice. *Plant Cell Environ.* **2021**, *44*, 948–963. [\[CrossRef\]](#)
40. Schwarz, M.A.D. *Comprehensive Natural Products Chemistry*; Sir Barton, D., Nakanishi, K., Meth-Cohn, O., Eds.; Pergamon: Berlin, Germany, 1999; pp. 367–400.

**Disclaimer/Publisher's Note:** The statements, opinions and data contained in all publications are solely those of the individual author(s) and contributor(s) and not of MDPI and/or the editor(s). MDPI and/or the editor(s) disclaim responsibility for any injury to people or property resulting from any ideas, methods, instructions or products referred to in the content.